ELSEVIER

Journal of Structural Geology xx (xxxx) 1–14

JOURNAL OF STRUCTURAL GEOLOGY

www.elsevier.com/locate/jsg

A direct method for modeling and unfolding developable surfaces and its application to the Ventura Basin (California)

Boris Thibert[a,*], Jean-Pierre Gratier[b], Jean-Marie Morvan[a,c]

[a]*Institut Girard Desargues, Université Claude Bernard, Lyon1, bat. 21 du Doyen Jean Braconnier, 69622 Villeurbanne Cedex, France*
[b]*Laboratoire de Géophysique Interne et Tectonophysique, Observatoire, CNRS-UJF, Géosciences, BP 51X 38041 Grenoble, France*
[c]*Geometrica's project, INRIA, 2004 route des Lucioles, B.P. 93, 06904 Sophia-Antipolis, France*

Received 23 October 2003; received in revised form 1 July 2004; accepted 11 August 2004

Abstract

In order to draw precise geological structures using scattered data, it is relevant to use criteria that integrate the kinematic properties of the structure. For example, developable folds can be selected by the observation of constant-length deformation markers. By establishing an accurate drawing of these folds, it is possible to precisely determine the geometrical limits of basin. We have developed a program, DEVELOPABLE-MESH, that integrates these developability criteria: this program first builds a 3D mesh using criteria that are based on the geometrical properties of developable surfaces; it then 'slightly' modifies the mesh to improve its developability; this mesh is finally unfolded. This program has been tested on a natural example of the lateral evolution of a thrust system to a fold structure (Red Mountain area in the Ventura basin). This particular structure has been already balanced by a trial and error method (UNFOLD program). This test confirms the validity of our approach: the DEVELOPABLE-MESH program builds near perfect developable folded surfaces. Therefore, it is geometrically coherent and can unfold these surfaces in a very short time. Moreover, the program is faster and can construct more complex developable surfaces than other conventional unfolding techniques based on a common interpolator.

Keywords: Developable; Mesh; Restoration; Unfold; Ventura Basin

1. Introduction

Data commonly available for drawing geological structures are generally either precise but very scattered (wells or boreholes) or continuous but rather approximate (geophysical data). Consequently, in order to draw precise geological structures, other information on the geological mechanism of structural development must be added to these data. This idea was a major breakthrough and was first introduced in the construction of geological cross-sections by the so-called 'cross-section balancing method' (Dahlstrom, 1969; Hossack, 1979). More recently, and in order to progress toward a true 3D balancing method, other techniques have been developed for balancing folded surfaces. At the present time, two types of folding mechanisms have been investigated, either shear deformation (Kerr et al., 1993) or flexural folding (Gratier et al., 1991). The interest of balancing developable surfaces is that the developability criterion is a strong constraint on the geometry of the strata. A surface is developable if it can be unfolded with length preservation into a flat surface (i.e. the surface is not 'stretched' in the process). Classical developable folds are class 1B fold (Ramsay, 1967), but there are several other mechanisms of folding. Actually, many layers do undergo area change during folding. However, most of the time it is not possible to evaluate the strain values along the layer. If strain values are not known the geometry of the geological structure can only rely on the geological and geophysical data and the balancing process cannot be done. It is worth noting that symmetrically, the local amount and distribution of strain

* Corresponding author. Correspondence address: Buck Institute For Age Research, 8001 Redwood Blvd, Novato CA 94945, USA
E-mail address: thibert@igd.univ-lyon1.fr (B. Thibert).

0191-8141/$ - see front matter © 2005 Published by Elsevier Ltd.
doi:10.1016/j.jsg.2004.08.011

cannot be calculated from the unfolding process because, when a non-developable surface is laid flat, the location and the characteristics of the residual strain depend on the path of the unfolding process. Integrating developable layers in surface balancing technique is possible even if there are only a few numbers of developable layers in the sedimentary pile. In fact, accurately drawing the geometry of certain developable layers is a strong constraint for the structural modeling of the whole sedimentary pile. But one must be very careful at identifying those developable layers. Developable layers are fairly easy to recognize by observing deformation markers (for example, fossils) showing no change in length along the neutral surface of the fold. This may be observed on samples removed, for example, from wells. The selection of a particular stratum that can be considered to be developable is therefore the result of careful observation of the folding mechanism and must be derived from true independent data. Relatively thin layers of carbonate rocks or sandstones are often pertinent. Faulting is not a problem if it remains possible to separate the whole folded competent layer into several patches of the developable layer. Patches are defined by faults and connected lines. Unfolding a thousand folded patches and restoring them along their faulted boundaries was done, for example, with this technique, for the Jura massif (Affolter and Gratier, 2004).

The problem of unfolding developable strata has been extensively studied: Gratier et al. (1991) and Gratier and Guillier (1993) developed the UNFOLD program to unfold meshes by laying the rigid triangles of this mesh flat and fitting them together by a least-square criterion. Lecomte et al. (1994) developed the PATCH program that uses spline functions to model strata and lay them flat like Bennis et al. (1991) did for other applications. The work of Sansom (1996), Rouby et al. (2000) and Williams et al. (1997) is also worthy of mention as they introduced complementary options. All these authors developed specific algorithms approximately following the best-fit mesh restoration principle. An alternative way proposed by Lévy and Mallet (1998) and Dunbar and Cook (2003) is to minimize the residual strain in the restored state. In this case the minimum strain criterion is analogous to and replaces the least-square fit criterion mentioned above. In all these methods, as in cross-section balancing, the process is a trial and error method. It is assumed that a balanced structure must be restorable to its initial undeformed state with respect to both the data and some additional constraints on the deformation mechanisms (as length preservation). Consequently, the initial geometry of the stratum has to be first established. Meshing with interpolation of raw data is an important step in the processing. It is generally necessary to smooth the raw data in order to avoid parasitic folds created by the program. This process may slightly shift the folded surface away from the raw data. This initial geometry is then unfolded. If the result is successful, for example, if the fitting criteria in the UNFOLD program are low enough (Gratier et al., 1991), the surface is considered to be a possible solution that is both compatible with the data and in agreement with the observed deformation mechanisms. If the fitting indicators are not sufficiently low, it may be necessary to redraw the surface. The whole trial and error process is rather time consuming.

A quite different approach is used in the present study. The aim is to directly draw surfaces that integrate the structural development mechanisms (the kinematic properties of the structures). A similar idea was used by Thibaut et al. (1996) to model fault surfaces. Observing that two solid rocks slipping on each other generate a thread surface, they modeled the fault surfaces by adding a thread criterion (i.e. a geometrical criterion) to the data. For the developable surfaces described in the present study, the idea is to focus directly on their 3D construction. To this end, the geometrical properties of developable smooth surfaces are integrated into the surface construction; a step to improve mesh developability is then added. The 3D mesh is therefore generally 'almost' developable (in the sense that its coefficient of length deformation is very small) and restoration of the mesh to its initial horizontal state is presumed to be easier than with other approaches. The aim is to skip the trial and error process and draw the developable surface directly.

Direct 3D construction of this type is also required in the modeling of mass transfer through sedimentary basins. Starting from true natural examples, two steps are needed (Cornu et al., 2002): a first step to restore the structure and assess the displacement field, and a second step to perform mass transfer forward modeling. In this case the geometry of the folded and faulted structure must be truly and directly restorable.

2. Characteristics of developable surfaces

The aim of this paper is to propose a mesh-type modeling process for developable strata. The geological property whereby a stratum is developable is linked to the geometrical property whereby the associated surface is developable.

In this part, after reviewing the main properties of smooth developable surfaces, some definitions relative to developable meshes are given. An example of a dome modeled by a developable mesh is then proposed. Finally, using an example, the importance of integrating geometrical properties of smooth surfaces (rules) in order to build reliable developable meshes is illustrated.

2.1. Developable smooth surfaces

S is assumed to be a smooth surface (i.e. locally parameterized by a function that can be differentiated twice) of the Euclidean space R^3. The surface S is assumed to be 'like a folded sheet of paper': it was initially flat and

has been deformed without changing the distances on the surface between every pair of points. In the language of differential geometry, such a surface S is said to be globally isometric to a flat surface. These surfaces have been extensively studied in mathematics (Hartman and Wintner, 1950, 1951; Hartman and Nirenberg, 1959). Despite their general interest, only a few studies have been undertaken in geology, as summarized in the work of Lisle (1992).

A remarkable property of this kind of surface has to do with Gaussian curvature. To explain this, certain notions of curvature are introduced. At a point p of a surface S, two lines of curvature $c_1(p)$ and $c_2(p)$ can be defined (Fig. 1a). The curvatures of these two lines at the point p are the principal curvatures $k_1(p)$ and $k_2(p)$. The Gaussian curvature of S at a point p is, by definition, $G_S(p) = k_1(p)k_2(p)$.

Although the two principal curvatures $k_1(p)$ and $k_2(p)$ of a surface at a point p are modified during isometric deformation, the Gaussian curvature $G_S(p)$ is constant (this is a consequence of Gauss's Theorema Egregium, which states that the Gaussian curvature is invariant under local isometry; see Do Carmo (1976) for instance). In the present case, this implies that the Gaussian curvature $G_S(p)$ at a point p is equal to the Gaussian curvature of a flat surface, that is to say zero. By definition, a surface is said to be developable if its Gaussian curvature is equal to zero.

It may be noted that, at each point p of a smooth developable surface S, at least one of the two curvatures $k_1(p)$ and $k_2(p)$ is equal to zero. Cones, cylindrical surfaces and tangential surfaces are classical examples of developable smooth surfaces (see Fig. 1c and Lisle (1992)). There is no general classification of developable surfaces. However, a smooth developable surface satisfies the following properties (see Hartman and Nirenberg (1959) for more details):

- For every point p in S, there exists a segment C_p, which is included in S and which contains p (see Fig. 1b). The segment C_p is called a rule.
- The direction of the normals along a rule C_p is constant.
- If the curvature of the surface S at a point p is not null, then the curvature of the surface S at every point of the rule C_p is not null.

The use of smooth developable surfaces for interpolating developable strata was considered, but interpolation with such surfaces is rather complex (for example, use of a spline function). On the contrary, meshes are well-suited to the problem:

– scattered data available in natural structures may be used to build a mesh,

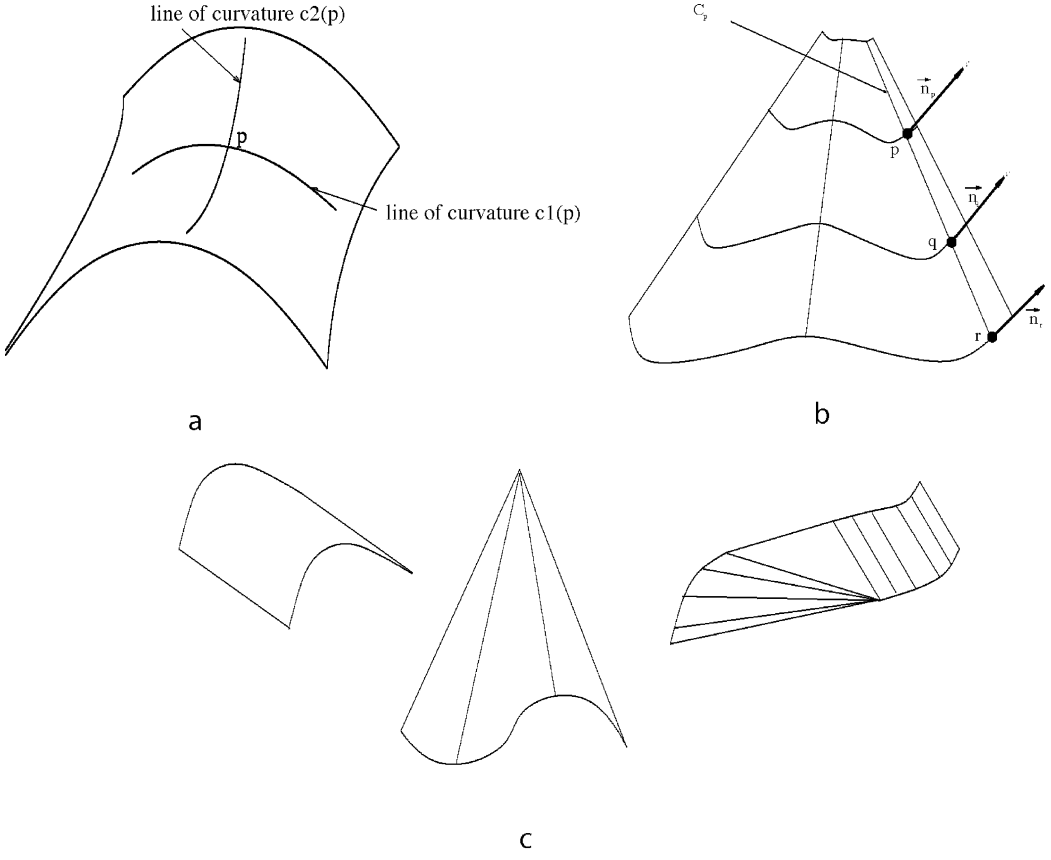

Fig. 1. Properties of smooth surfaces. (a) The two lines of curvature passing through a point p of a smooth surface. (b) Some properties of developable smooth surfaces: for every point p, there exists a segment C_p that is included in the surface and which contains p; the normal to the surface is constant along C_p. (c) Examples of smooth developable surfaces: the cylinder, the cone, and a combination of planar/cylindrical/conical surface.

– the developability criterion is quite easy to define on a mesh,
– mesh unfolding is fast.

2.2. Developable meshes

It is assumed here that T is a mesh (i.e. a surface composed of triangles such that the intersection of two triangles is empty or equal to an edge or equal to a vertex). Moreover, it is assumed that T is also globally isometric to a flat mesh (it can be unfolded without changing the distances of the curves).

As in the smooth case, this property relates to Gaussian curvature. Aleksandrov and Zalgaller (1967) defined the Gaussian curvature $G_T(p)$ of T at a vertex p as being the angular defect to 360° (see Fig. 2a). If the mesh T is globally isometric to a flat surface, then its Gaussian curvature is equal to zero at each interior vertex. As in the smooth case, mesh is said to be developable if its Gaussian curvature is equal to zero at each interior vertex.

A new notion is introduced, related to the discrete Gaussian curvature. Let S_p be a curve of T composed of points that are at a distance r from the vertex p. If r is small enough, the length of this curve is exactly $l = \alpha r$ (where α is the sum of the angles at the vertex p in radians). If the mesh T is developable, then this length is exactly $l_{\text{dev}} = 2\pi r$. Therefore, the coefficient of length deformation (see Fig. 2b and c) is defined by:

$$\text{coef}(p) = \frac{l - l_{\text{dev}}}{l_{\text{dev}}} = \frac{\alpha r - 2\pi r}{2\pi r} = \frac{G_T(p)}{360}.$$

2.3. Modeling a dome

Dome structures are very common in petroleum studies and can function as oil traps. It is often assumed that such a structure necessarily develops with surface length change. However, a dome structure can also be a true developable surface without any surface length change. Fig. 2d shows an example of a folded sheet of paper that models a dome with kink structure. Such a structure must always include a non-convex area; from the top vertex, a valley must lie between two edges.

2.4. Fitting a developable surface to a cloud of points

Consider the following problem: a cloud of points is given (based on an unknown smooth surface S) and a mesh based

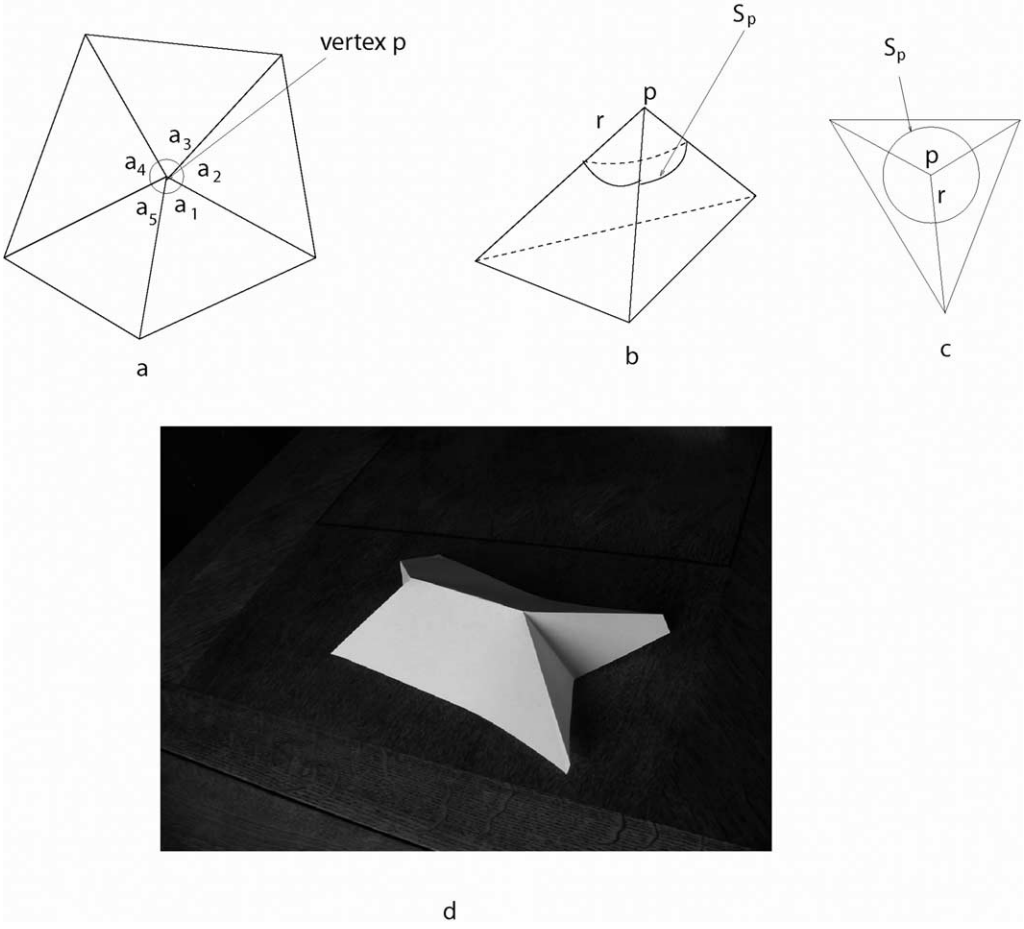

Fig. 2. Meshes. (a) The Gaussian curvature (i.e. the angular defect) at a vertex p of a mesh T: $G_T(p) = 360 - (a_1 + a_2 + a_3 + a_4 + a_5)$. (b) The curve S_p composed of every point that is at a distance r from a vertex p of a mesh T. (c) The curve S_p in the case where T is a flat mesh. (d) A folded sheet of paper.

on these points must be built with the mesh geometry being 'close' to the geometry of *S*. Of course, there are many possible meshes containing these points. Even if the constraint of being developable is added, there are still many meshes containing these points and that have different geometrical properties.

To illustrate this phenomenon, the following example has been built (see Fig. 3): a cloud of points belonging to a half-cylinder is considered (Fig. 3a) and two developable meshes are built whose vertices are exactly these points (Fig. 3c and e). The mesh of Fig. 3c is half a Schwarz lantern (which is a well-known example). Since the two meshes and the half-cylinder are developable, they are unfolded. Note that the unfolded surfaces of the two meshes are very different: the unfolded mesh 3f is close to the unfolded half-cylinder (Fig. 3b) while the unfolding of the half Schwarz lantern (Fig. 3d) results in a very different form from the unfolded half-cylinder. This phenomenon is more striking when the number of vertices is increased (Morvan and Thibert, 2002).

It is worth noting that, in this example, the geometry of the mesh in Fig. 3e is close to the geometry of the smooth developable surface, in the sense that many edges of the mesh in Fig. 3e are 'rules' of the half-cylinder (i.e. segments included in the half-cylinder). This is not the case for the mesh in Fig. 3c: no edge in the mesh in Fig. 3c corresponds to the 'rules' of the half-cylinder.

Therefore, the idea of the algorithm proposed here is to

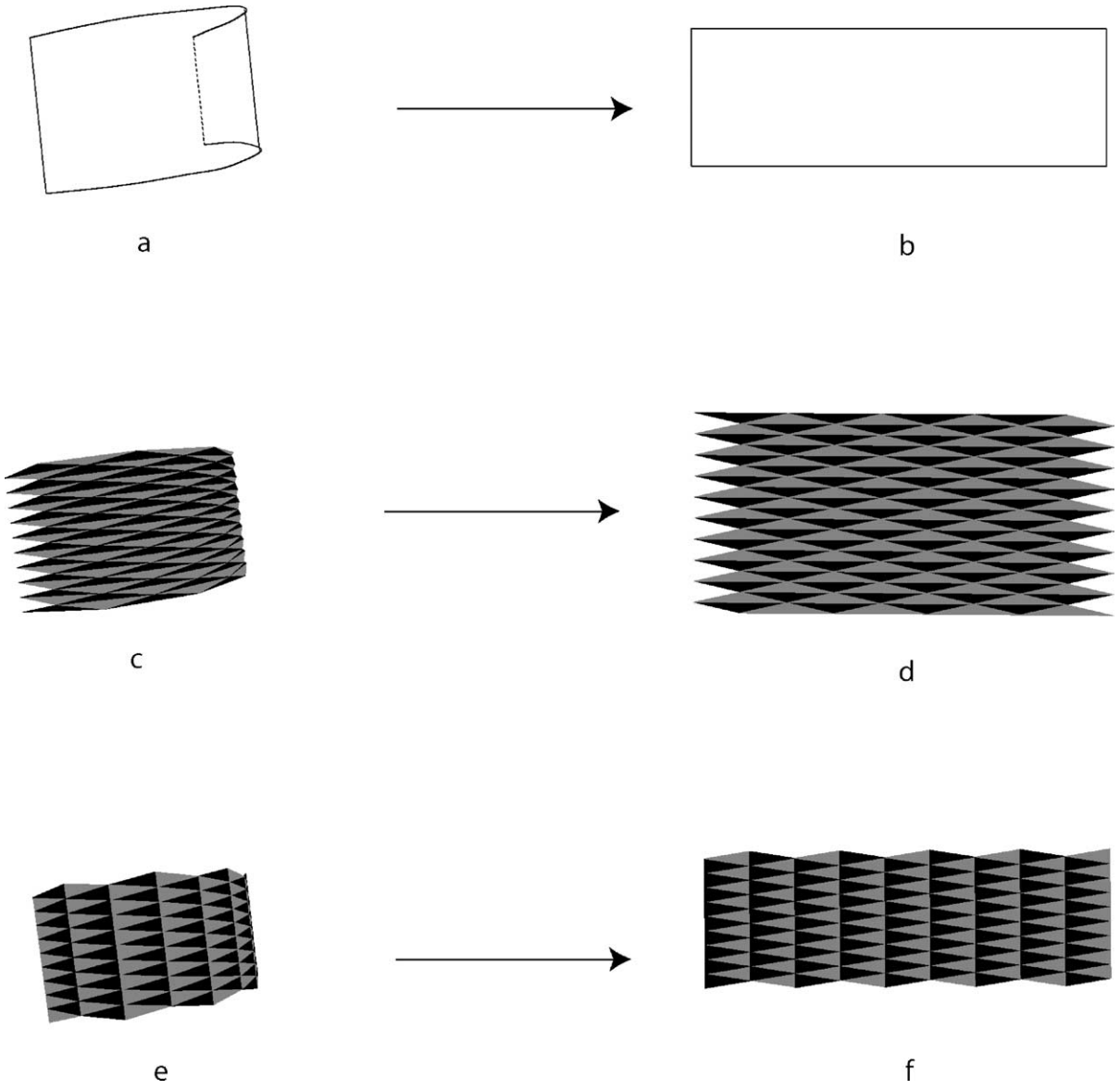

Fig. 3. Two meshes with the same set of vertices of half a cylinder. (a) Half a cylinder. (b) Unfolding of the half cylinder. (c) Half a Schwarz lantern in which the vertices belong to the half cylinder. (d) Unfolding of the half Schwarz lantern. (e) A mesh in which the vertices are exactly the vertices of the half Schwarz lantern. (f) Unfolding of the mesh in (e).

integrate geometrical properties of developable meshes into mesh construction in order to build reliable, developable meshes.

3. Construction of developable meshes

This part explains the construction of developable meshes and their unfolding. The algorithm of the DEVELOPABLE-MESH program is described. This algorithm is composed of:

- A sub-routine *Triangulate*, which builds a mesh using certain geometrical properties of developable meshes (Section 3.1).
- A sub-routine *Modify*, which optimizes the developability of a mesh by 'slightly disturbing' it (Section 3.2).
- A sub-routine made by Sheffer and De Sturler (2001), which unfolds a mesh (Section 3.3).

3.1. Construction of a mesh (Triangulate sub-routine)

The key idea of the algorithm is to integrate geometrical properties of developable surfaces in the mesh construction. More precisely, using the properties of developable smooth surfaces introduced in Section 2.1 (and in Fig. 1b), two kinds of areas are determined:

- areas where the surface is flat or cylindrical;
- areas that are not flat and for which certain rules C_p are determined.

Algorithm inputs: the input data are composed of:

- A family of level set curves $C_1,\ldots,C_n$ (see Fig. 4a for instance). The curves C_i represent strike-lines. Each curve C_i is polygonal and is included in a horizontal plane '$z=$ constant'. The orthogonal projections of any two level set curves in the plane '$z=0$' do not intersect.
- A closed plane curve B (polygonal) in the plane '$z=0$'.
- A family of parameters linked to notions of scale and tolerated errors.

Output: The output is a mesh T, the orthogonal projection of which onto the plane '$z=0$' is a mesh of boundary B.

Sketch of the Triangulate sub-routine algorithm (3 steps):

1. The algorithm determines 'areas' where the surface seems to be cylindrical or flat. During this step, some edges of $C_1,\ldots,C_n$ are removed where the surface seems to be flat or cylindrical and are replaced by other edges (bold edges in Fig. 4b) that are assimilated to 'flat zones'. C denotes the set of new edges (bold edges in Fig. 4c).
2. The algorithm then determines 'areas' where the surface is curved (bold edges in Fig. 4d) and determines certain surface rules. During this step, some edges are added to the set of edges C: these edges are assimilated to surface 'rules' (bold edges in Fig. 4f).
3. The algorithm finally builds a mesh T so that the edges of C belong to T and so that the orthogonal projection of T on the plane '$z=0$' is a mesh of boundary B.

Details of the three steps of this algorithm are given below, and especially steps 1 and 2, which use the geometrical properties of developable surfaces.

3.1.1. Determination of flat or cylindrical 'zones' (Step 1)

If a plane S is cut by two parallel planes (which are not parallel to S), it produces two segments that are parallel. If a horizontal cylinder S is intersected by two horizontal planes, it also produces two segments that are parallel.

Therefore, to mimic the smooth case, pairs of parallel segments must be determined (by using the set of level curves, see Fig. 4a). Each pair will be assimilated to a 'flat zone' (see Fig. 4c).

Sketch of the algorithm of Step 1:

This algorithm depends on three parameters. Two parameters k_S and e_p are linked to tolerated errors and one parameter L_S is linked to a notion of scale.

(a) Determination of 'straight zones': for every planar polygonal curve C_i, every piece of 'straight zone' (i.e. a zone of length greater than L_S and such that the sine of the angle between the normal of two edges of the zone is less than k_S) is 'replaced' by a segment (Fig. 4b).
(b) Determination of pairs of 'parallel straight zones': each set of two segments determined in Step 1(a) is checked to see whether they are 'almost parallel' (i.e. whether the sine of the angle between the two segments is less than e_p) and 'close' to each another.
(c) Elimination of segments with orthogonal projection in the plane '$z=0$' intersect: if two segments have intersecting projections, they are 'shortened' so as to remove the intersection.

Fig. 4. Algorithm of the *Triangulate* sub-routine (all the polygonal level curves are seen from above—they do not lie in the same horizontal plane). (a)–(c) Step 1. (a) The initial level curves C_i. (b) Every 'straight zone' is replaced by a long segment (shaded). (c) The 'flat zones' (shaded). (d)–(f) Step 2. (d) 'Curved zones' on every level curve C_i. (e) A family F of triplets of 'curved zones'. (f) The segments (associated with the rules) added to the set of edges C. (g) Explanation of the normal criterion: if S is a smooth developable surface, then the normals $P(\vec{n}_i)$ to level curves C_i along a rule C_p have the same direction. (h) The normal criterion is satisfied because the normals of the three zones z_i are close to one another (but the alignment criterion is not satisfied). (i) The convexity criterion is not satisfied (because it is not satisfied for the two zones v_1 and u_2). (j) The convexity criterion is satisfied (but the alignment criterion is not satisfied). (k) A family of triplets of 'curved zones' that satisfies all the criteria. (l) A family of triplets of 'curved zones' that does not satisfy the non-intersection criterion (because the orthogonal projections of the two segments $[p_1, q_2]$ and $[p_2, q_1]$ on the plane '$z=0$' intersect).

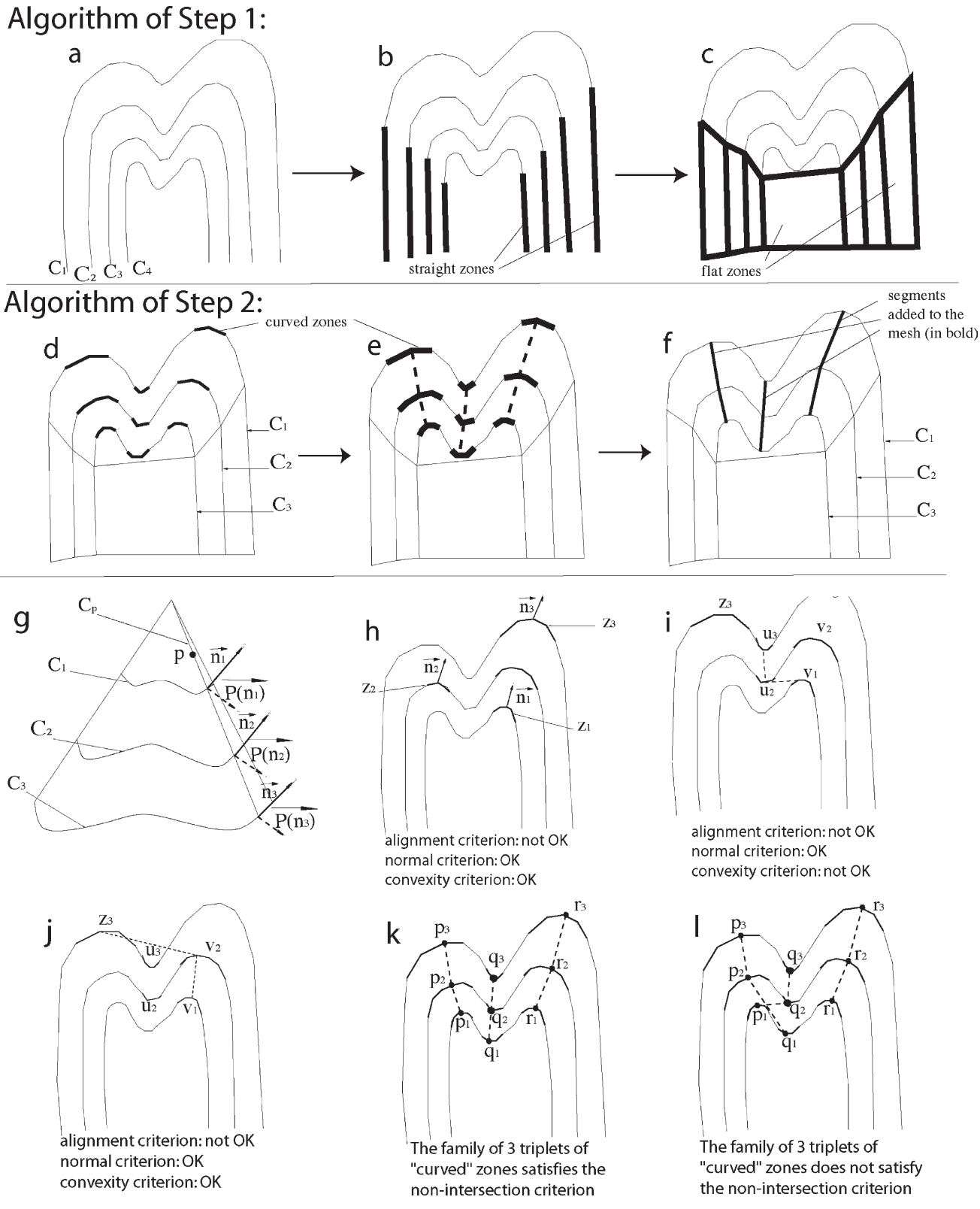
Algorithm of Step 1:
a
b
c
C1 C2 C3 C4
straight zones
flat zones
Algorithm of Step 2:
curved zones
segments added to the mesh (in bold)
d
e
f
C1
C2
C3
g
h
i
alignment criterion: not OK
normal criterion: OK
convexity criterion: OK
alignment criterion: not OK
normal criterion: OK
convexity criterion: OK
j
k
l
alignment criterion: not OK
normal criterion: OK
convexity criterion: OK
The family of 3 triplets of "curved" zones satisfies the non-intersection criterion
The family of 3 triplets of "curved" zones does not satisfy the non-intersection criterion

(d) Each pair of 'parallel straight zones', is associated with a closed polygonal curve composed of four vertices (Fig. 4c). This curve is assimilated to a 'flat zone' because the four vertices are 'almost' planar. All the edges of the closed polygonal curves are added to the set C.

3.1.2. Determination of segments (assimilated to 'rules') (Step 2)

Using the set of level curves (Fig. 4d), the aim is to determine a set of segments (assimilated to 'rules'). The idea is first of all to 'gather' zones z_i, z_j, z_k of level curves (respectively, C_i, C_j, C_k); then, two segments $[p_i, p_j]$ and $[p_j, p_k]$ (where p_i is a vertex of the zone C_i) are associated with each triplet of zones (z_i, z_j, z_k). These segments are added to the set C.

The determination of the triplets (z_i, z_j, z_k) is based on the geometrical properties of developable smooth surfaces (see the Proposal in Section 2.1 and Fig. 4g) and integrates the following criteria:

1. Curvature criterion: 'zones' are gathered for which the 'curvature' is larger than a value β fixed by the user.
2. Normal criterion: 'zones' are gathered for which the normals are close (the explanation of this criterion is illustrated in Fig. 4g; an example of a triplet (z_i, z_j, z_k) satisfying this criterion is given in Fig. 4h).
3. Convexity criterion: 'zones' are gathered which have a similar convexity (locally on the same side of their oriented normal; see Fig. 4j).
4. Non-intersection criterion: we gather 'zones' whose orthogonal projections onto the plane '$z=0$' do not intersect (see Fig. 4k).
5. Alignment criterion: 'zones' are gathered, which are aligned along the same segment (for example, this criterion is satisfied in Fig. 4k and not in Fig. 4l).
6. Neighborhood criterion: 'zones' are gathered, which belong to level curves that are close to one another (for example, in Fig. 4d, the three level curves C_1, C_2 and C_3 satisfy this criterion because there is no level curve between C_1 and C_2 and between C_2 and C_3).

Sketch of the algorithm of Step 2 (Fig. 4d–f):

This algorithm depends on eight parameters. The parameters β, p_a, p_n, p_c, α_a, α_n, α_c, k_c are linked to tolerated errors and the parameter L_c is linked to a notion of scale.

(a) Determination of 'curved zones': for every planar polygonal curve C_i, zones of length less than L_c are determined and along which the normal varies by more than a minimum angle k_c.

(b) For every triplet of planar polygonal curves C_i, C_j, C_k (satisfying the neighborhood criterion):

(b.1) All the families $F=\{(z_i, z_j, z_k)\}$ of triplets of 'curved zones' (where $z_i \subset C_i$) compatible with the non-intersection criterion are determined.

(b.2) For every family F, all the triplets $r=(z_i, z_j, z_k)$ are removed so that:

$$E_a(r) > \alpha_a$$

or

$$E_n(r) > \alpha_n$$

or

$$E_c(r) > \alpha_c,$$

where E_a is an error function measuring the alignment of the three zones of r, E_n is an error function measuring whether the normals of the three zones are close and E_c is an error function measuring whether the three zones have a compatible convexity.

(b.3) For every family of triplets of 'curved zones' F, the following error is calculated:

$$E(F) = \sum_{r \text{ triplet of } F} p_a E_a(r) + p_n E_n(r) + p_c E_c(r)$$

where p_a, p_n and p_c are the weights associated with the alignment, normals and convexity errors.
Only the family F of triplets with minimum error $E(F)$ is retained.

(b.4) Two segments $[p_i, p_j]$ and $[p_j, p_k]$ (which are put in the set C; see Fig. 4f) are associated with each triplet $r=(z_i, z_j, z_k)$ of F.

3.1.3. A constrained mesh (step 3)

At this stage of the construction, a mesh has not yet been defined, but only a set of vertices V and a set of segments S created by the two first steps of the algorithm (and also containing, respectively, the vertices and edges of the plane curve B).

This step shows how to build a mesh in which the set of vertices contains V and the set of edges contains S. The classical *Constrained Delaunay Triangulation* theory is used. However, this particular triangulation only exists in 2D (and not in 3D). Therefore, the procedure used is as follows:

1. First the constraints V and S are projected onto the horizontal plane '$z=0$'.
2. Then, using the *Constrained Delaunay Triangulation* algorithm (implemented in the library CGAL), a 2D triangulation is built in which the set of vertices contains

the projection of V and the set of edges contains the projection of S.
3. The triangles that are outside the plane curve B are then deleted.
4. Finally, all the vertices of the mesh are raised.

Note that the construction of a mesh is based on properties of developable smooth surfaces. However, it is not necessarily developable in general. This explains why it is necessary to modify the mesh T so as to make it developable (or 'almost' developable).

3.2. Optimization of mesh developability (Modify sub-routine)

The mesh produced by the *Triangulate* sub-routine is not developable in general. Consequently, a sub-routine is proposed here that decreases the coefficient of length deformation (see Fig. 2b and c) of a mesh by 'slightly disturbing' it. Two algorithms disturbing a mesh iteratively are proposed (the user can use one or both of them):

- an algorithm that modifies the position of the vertices (Section 3.2.1),
- an algorithm that 'flips' some edges (Section 3.2.2).

3.2.1. Modification of vertex position:

This algorithm depends on two parameters r and h. Parameter r governs the size of a neighborhood of every vertex of the mesh. Parameter h is related to the distance between two positions that a vertex of the mesh can have.

In this algorithm, a mesh T is modified iteratively. A sequence of meshes T_n is built in the following manner: let $T_0 = T$; at step n, a vertex p of the mesh T_n is chosen at random. Two choices (fixed by the user) are available for calculating its new position:

1. Either random choice of the new position of the vertex p in the neighborhood of the vertex of the initial mesh T_0,
2. Or choice of the new position in the 3D direction that locally minimizes the Gaussian curvature of T_n at the vertex p. This direction is given by the vector (calculated by Desbrun et al. (2002)):

$$\nabla_p G_{T_n}(p) = \sum_{q \text{ neighbor of } p} \frac{\cot\alpha_{1,pq} + \cot\alpha_{2,pq}}{\|p-q\|^2}.$$

The line L_p spanned by the vertex p and the vector $\nabla_p G_{T_n}(p)$ is determined (Fig. 5a). The new position of p is on the line L_p at a distance h from p (if the new position is not too far from the position of the vertex p of the initial mesh T_0).

Then, let $\bar{T}_n$ denote the mesh T_n for which the position of the vertex p has been changed. If $\sup_{p\in\bar{T}_n} |G_{\bar{T}_n}(p)| \leq \sup_{p\in T_n} |G_{T_n}(p)|$, then $T_{n+1} = \bar{T}_n$ is chosen, otherwise $T_{n+1} = T_n$ is chosen.

3.2.2. Flipping some edges of the mesh

In this algorithm, a mesh T is iteratively modified without changing the position of its vertices. Only some edges are flipped. The sequence of meshes T_n is built in the following manner: let $T_0 = T$; at step n, an edge $[p_n, q_n]$ of the mesh T_n is chosen at random (see Fig. 5b). If the triangles $r_n s_n q_n$ and $p_n s_n r_n$ do not exist and if $\alpha_1 + \alpha_2 < \pi$ and $\beta_1 + \beta_2 < \pi$, then the edge $[p_n, q_n]$ is flipped into the edge $[r_n, s_n]$. The new mesh is denoted by $\bar{T}_n$.

If $\sup_{p\in\bar{T}_n} |G_{\bar{T}_n}(p)| \leq \sup_{p\in T_n} |G_{T_n}(p)|$, then $T_{n+1} = \bar{T}_n$, is chosen, otherwise $T_{n+1} = T_n$ is chosen.

3.3. Unfolding

The two sub-routines *Triangulate* and *Modify* build a mesh that is not developable in general, but in which the coefficient of length deformation coef(p) is 'small' for every vertex p (this coefficient measures the non-developability of a mesh). Therefore the mesh is 'almost' developable and it is possible to unfold it. However, since it is not completely developable, it cannot be unfolded directly: it was decided therefore to use a program developed by Sheffer and De Sturler (2001) based on a global method.

Their algorithm uses the following idea: if all the angles of a flat mesh and the length of one edge are known, then the flat mesh can be reconstructed. Therefore, by minimizing the energy linked to the deformation of the angles, the algorithm of Sheffer and De Sturler (2001) builds a family of angles that satisfies the constraints linked to flat meshes, from which a flat mesh can be reconstructed.

4. Application to the Ventura Basin

The Ventura basin is an area of oil fields that have been intensively drilled. For example, by studying thousands of oil wells onshore, the Ventura Basin Study Group built up numerous cross-sections connecting the wells (Hopps et al., 1995). This database is available on the web site of the UCSB (http://www.crustal.ucsb.edu/projects/hopps/). Other data were gathered from several offshore and onshore studies (Jackson and Yeats, 1982; Yeats, 1983; Hupfile, 1991; Heck, 1998; Sorlien and Kamerlin, 1998; Kamerlin and Sorlien, 1999). All these data were used to study the 3D lateral evolution of a large thrust system (Red Mountain Thrust) into a regional fold (Fig. 6). In such a non-cylindrical structure, the balanced cross-section technique cannot be applied since the basic assumptions (parallel displacements) are not respected. In such a case, the balanced map technique can be used in order to test the possible unfolding of a reference layer. As summarized in the introduction, map-balancing method comprises several steps. The initial geometry of the

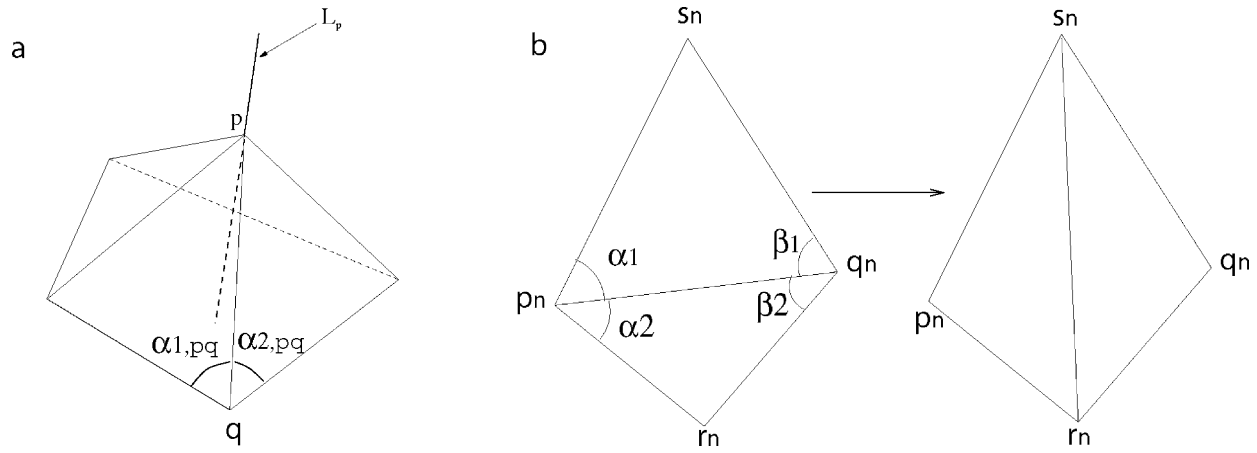

Fig. 5. Algorithm of the *Modify* sub-routine. (a) The direction that locally optimizes the Gaussian curvature at the vertex p is the line L_p spanned by the vector $\nabla_p G_{T_n}(p)$. (b) Flipping of the edge $[p_n, q_n]$.

structure, mostly in the form of a structure contour map, must be drawn up in all cases.

This first step was completed for the same horizon over the entire area (Vaqueros Formation made up of a thin layer of dolomite). This involved extrapolating the data both below the level of the deepest oil well and above the present erosion level in the cross-section (Fig. 6). To this end, the shape of the folds was measured in areas with a good data coverage. It was found that, when considering a large part of the series (several thousand meters thick) the folds are of class 1C type (Ramsay, 1967). In more detail, this general shape is a combination of class 1B folds (constant thickness folded layers = competent layers = Vaqueros Formation) and class 2 folds (similar folds = incompetent layers). Consequently, class 1C rules were used to extrapolate the general shape of the competent layer (Vaqueros formation) that is likely to

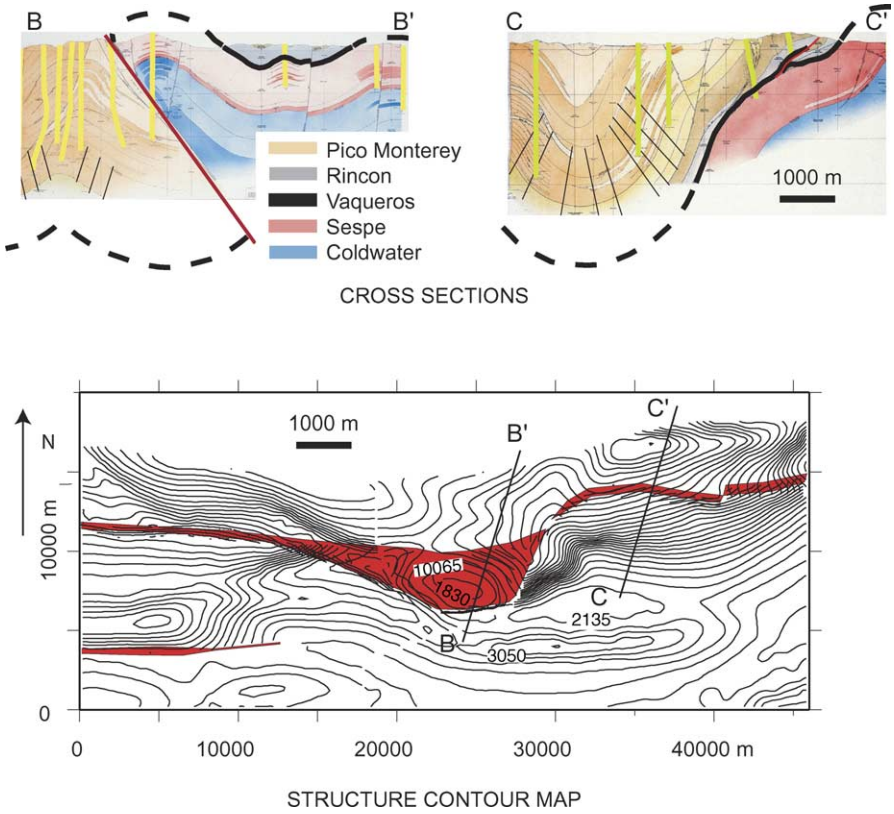

Fig. 6. Data on the Red Mountain Thrust: two examples of the numerous cross-sections and the balanced structure contour map (all positive contour lines indicated in meters refer to a reference plane 0 located at −9150 m). The yellow lines are the trace of the wells. Fold shape analyses based on equal line curvature (black lines) show how the geometry of the strata has been derived from the data on cross-sections. The names of folds and faults are labeled in Fig. 7. Red areas correspond to the map view of thrusts and backthrust (see Fig. 7).

have been deformed with constant thickness (see Fig. 6). The structure contour map was digitized (Fig. 6). The initial stratum has been broken up into six different pieces, called patches, defined by faults and connecting lines. The two following types of map restoration method for each patch were then used:

- The UNFOLD program allows the geometrical compatibility of the surface to be tested using a trial and error method (Gratier et al., 1991). This technique has been widely presented in previous papers, including an application to the entire Los Angeles and Ventura basin (Gratier et al., 1999) and will not be detailed here. The initial surface is meshed by rigid triangles using the GMT gridding function; the rigid triangles are then laid flat consecutively with the position of each triangle versus their neighbors determined by a least-squares method. Successive iterations are carried out until pertinent values of the fitting parameters are reached. However, the set of triangles obtained does not form a mesh; it is a network of best-fitted triangles. Fitting indicators give information on the developability of each unfolded patch; then the unfolded patches of stratum are fitted along the faults. If it cannot be successfully restored, the structure is redrawn as many times as necessary (Gratier and Guillier, 1993).
- The DEVELOPABLE-MESH program starts from the same initial set of data (structure contour map). However, after mesh building, a step is added that tries to improve mesh developability. If successful, this step allows a near perfect developable mesh to be built. Consequently, the restoration of the mesh to its initial horizontal state is presumed to be much easier than with the UNFOLD method.

For the UNFOLD technique, the GMT system was used in order to grid the surface. The UNFOLD program was then used without too many problems. Most of the folded surfaces were unfolded with sufficiently low fitting indicator values to support the assumption of developable surfaces. However, one patch—stratum 3—could not be unfolded directly and had to be divided into two patches that were unfolded independently and fitted together. When all the blocks were unfolded, the best fit of the unfolded blocks was made with a graphic interactive system (the unfolded patches were adjusted to one another 'by hand' using rotations and translations). The first structure contour map was not perfect. The geometry of the faults was corrected in order to minimize the voids and overlaps between the unfolded blocks. Most of the problems derived from the initial geometry of the Rincon fault and from the Red Mountain fault (in its zone of maximum displacement). Most of the misfits were corrected in the last version of the surface horizon which is given in Fig. 7 as a perspective view (top) and map views of both the deformed (present) state and undeformed (restored) state, with indication of the relative displacement field from one state to the other (the southern boundary being considered as fixed).

It is interesting to note that the displacement value is fairly constant all along the transition between the most discontinuous deformation (Red Mountain Thrust) and the most continuous one: Sulphur Mountain Fold (east) and the Carpentaria Fold (west). In both cases, however, back thrusts (Rincon to the west, Sisar and Big Canyon to the east), contribute to the shortening of the folded structure helping to equalize the displacement values all along the transition between the main thrust and the folds. This transition between the main thrust and the folds is associated with 'buttonhole tear faults': faults that have their two tips points localized within the studied area. Along strike variations are observed along the faults. They are accommodated both by the folding and the faulting processes. The accuracy of the global fitting is here a good test of the compatibility of the deformed structures.

The DEVELOPABLE-MESH program was used and will be especially detailed for the patch of stratum 3 that was difficult to unfold with the UNFOLD program.

It is possible to visualize the data, which consist of a structure contour map of the patch of stratum 3 (Fig. 8a and b) and a plane-closed curve forming the boundary of the mesh projection (Fig. 8c). Using these data, the DEVELOPABLE-MESH program produces a mesh (Fig. 8f and g) that is 'almost developable' (the maximum length deformation for a vertex is 1% and the average length deformation per vertex is 0.1%). Therefore, this mesh is unfolded directly by the sub-routine of Sheffer and De Sturler (2001) in Fig. 8h. Note that there is no need to divide the patch of stratum 3 into two meshes, to unfold both meshes separately and then to fit them together after unfolding as was necessary with UNFOLD.

The intermediate steps of the DEVELOPABLE-MESH program concerning the patch of stratum 3 can be visualized. In Fig. 8d, the 'flat zones' and the 'rules' determined during the two first steps of the *Triangulate* sub-routine are visualized. Fig. 8e also shows the mesh produced by *Triangulate* (before optimization of the developability). This mesh is then slightly modified by the *Modify* sub-routine (Fig. 8f). The developability errors are also shown in Fig. 8g.

The five other patches of strata have also been modeled and unfolded with DEVELOPABLE-MESH. The intermediate results concerning these patches have not been shown, but it is worth noting that their length deformation is small: for each patch, the maximum length deformation for a vertex is less than 1.8% (and is less than 0.5% for two patches) and the average length deformation per vertex is less than 0.13%.

It is interesting to note that the shapes of the six patches are coherent: the patches can be adjusted to one another 'by hand' (using rotations and translations with a simple interactive graphic program). The initial stratum was therefore restored by gluing the six patches together (Fig. 8i).

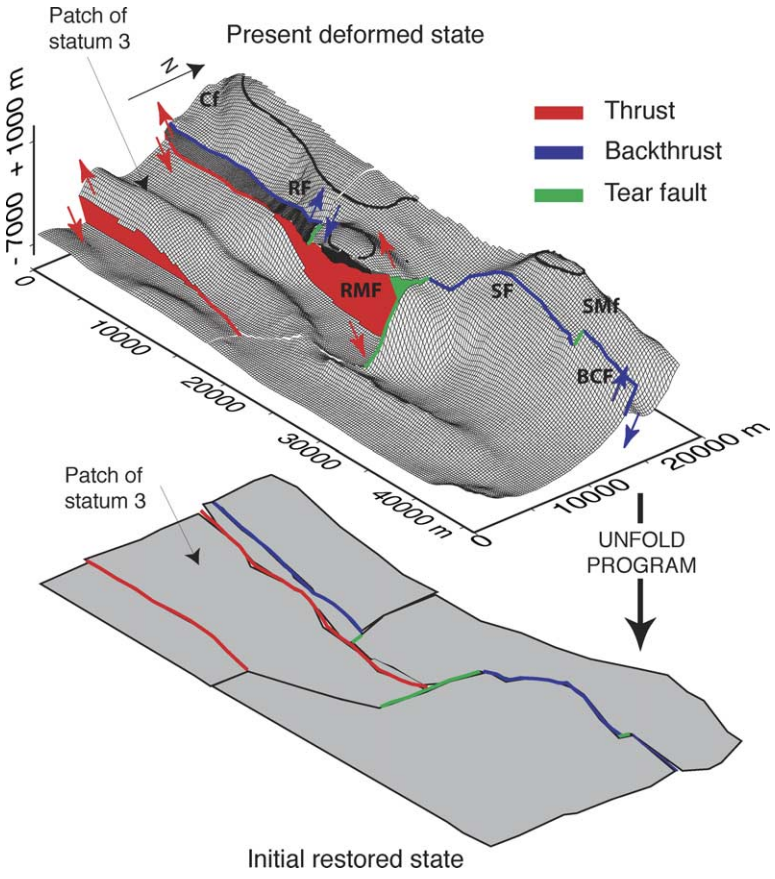

Fig. 7. Modeling the Red Mountain Thrust area using the UNFOLD program: perspective view of the present deformed state (top) and the initial restored state (bottom). Names of faults and folds: RMF = Red Mountain fault, RF = Rincon Fault, SF = Sisar Fault, BCF = Big Canyon Fault, SMf = Sulphur Mountain fold, Cf = Carpenteria fold.

5. Discussion

The unfolded patches obtained with DEVELOPABLE-MESH are very similar to those obtained with UNFOLD. However, several differences can be noted between the two programs.

First, UNFOLD does not allow the patch of stratum 3 to be unfolded in one piece (it had to be divided into two patches that were unfolded independently and fitted together). DEVELOPABLE-MESH builds and unfolds the six patches of strata without any problem.

The 3D meshes produced by DEVELOPABLE-MESH are 'almost developable' (in the sense that the length deformation is, for example, for the stratum 3, less than 1% for every patch with average length deformation per vertex of 0.1%).

The DEVELOPABLE-MESH program is based on geometrical properties of developable smooth surfaces: it determines 'zones' with characteristics of developable smooth surfaces. From an opposite viewpoint, it depends on several parameters (that are linked to tolerated errors and to the scale of data).

It is worth noting that the choice of developable layers is a crucial parameter. So, the interest of adding such a constraint relies on the quality of the geological analysis.

The main interest of this new program is to allow a direct construction of developable surfaces. This has several advantages. The first one is to gain time in processing the data when this program is used in order to restore the folded structures to their initial state. The second one is to use this program in 3D numerical models of fluid transfer within deformed sedimentary basin. With such a modeling, the present (deformed) state is first restored backward to its initial state. Then a forward modeling is done in order to study fluid transfer through the progressive deformation. The use of one or two developable layers in the sedimentary pile allows a direct backward restoration without the drawbacks of the trial and error approach that is needed with the classical methods of unfolding.

6. Conclusion

The DEVELOPABLE-MESH program models developable strata in 3D by using both scattered data and geometrical properties of developable smooth surfaces. The program comprises three steps: Step 1 builds a mesh using certain geometrical properties of developable meshes; Step 2

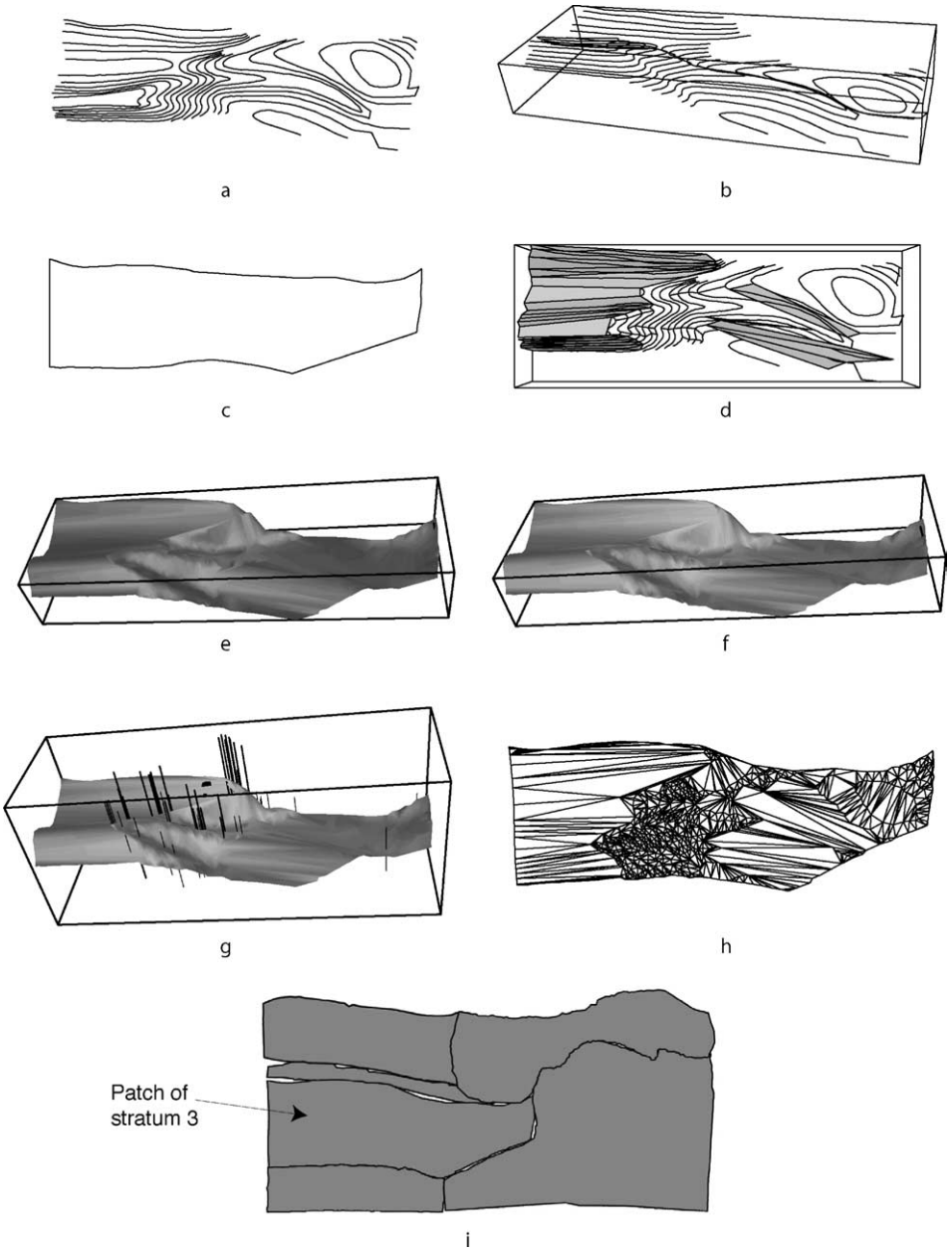

Fig. 8. Modeling the Red Mountain Thrust using the DEVELOPABLE-MESH program. See Fig. 7 for the names of the structures. (a) The level curves (structure contour map) of the patch of stratum 3 seen from above. (b) The level curves of the patch of stratum 3. (c) The closed curve (that will be the projection of the patch of stratum 3). (d) The 'flat zones' and the rules (segments) determined by the *Triangulate* sub-routine. (e) The mesh obtained by the *Triangulate* sub-routine.(f) The mesh obtained after disturbance using the *Modify* sub-routine. (g) Visualization of the coefficient of length deformation (for every vertex p, $\mathrm{coef}(p) < 1.05\%$); if a vertex p satisfies $0.28\% < \mathrm{coef}(p) < 0.83\%$, then there is a thin vertical segment; if a vertex p satisfies $0.83\% < \mathrm{coef}(p) < 1.05\%$, then there is a thick vertical segment. (i) Restoration of the initial state.

optimizes the developability of the mesh by 'slightly disturbing' it; Step 3 unfolds the mesh.

DEVELOPABLE-MESH was tested on the natural example of the lateral evolution of a thrust system to a fold structure (Red Mountain in the Ventura basin). Such a structure was first balanced by a trial and error method (UNFOLD). The transition between the main thrust and the folds was found to be associated with 'buttonhole tear faults' localized within the area studied.

The restoration of every patch of the stratum and the fact that the previously balanced patches can be fitted easily together would appear to validate this program. Due to the direct construction that includes developability criteria, the DEVELOPABLE-MESH program built meshes that have a small coefficient of length deformation (i.e. 'almost developable'). It also ran faster and allowed more complex developable surfaces to be constructed than other unfolding techniques that use a common interpolator.

Acknowledgements

We thank M. Ford and J. Dunbar for their fruitful review and D. Ferrill for his final help. Studies in California were supported by the Southern California Earthquake Center and the Institute for Crustal Studies, UC Santa Barbara. We thank T. Hopps, M. Kamerlin, C. Nicholson and C. Sorlien for their help in gathering the data.

References

Affolter, T., Gratier, J.P., 2004. Map-view retrodeformation of an arcuate fold-and-thrust belt: the Jura case study. Journal of Geophysical Research 109 (B3), 31–50.

Aleksandrov, A.D., Zalgaller, V.A., 1967. Intrinsec Geometry of Surfaces. American Mathematical Society, Providence, Rhode Island. 327pp.

Bennis, C., Vézien, J.M., Igésias, G., 1991. Piecewise surface flattening for nondistorted texture mapping. Computer Graphics 25, 237–246.

Cornu, T., Schneider, F., Gratier, J.P., 2002. 3D kinematic modeling of sedimentary basin deformation, in: Nieuwland, D.A. (Ed.), New Insights into Structural Interpretation and Modeling Geological Society Special Publication, 212, pp. 275–283.

Dahlstrom, C.D.A., 1969. Balanced cross-sections. Canadian Journal of Earth Science 6, 743–757.

Desbrun, M., Meyer, M., Alliez, P., 2002. Intrinsec Parameterizations of Surface Meshes. Eurographics's Conference Proceedings, pp. 209–218.

Do Carmo, M.P., 1976. Differential Geometry of Curves and Surfaces. Prentice-Hall, Englewood Cliffs, New Jersey. 745pp.

Dunbar, J.A., Cook, R., 2003. Palinspastic reconstruction of structure maps: an automated finite element approach with heterogeneous strain. Journal of Structural Geology 25, 1021–1036.

Gratier, J.P., Guillier, B., 1993. Compatibility Constraints on Folded and Faulted Strata and Calculations of Total Displacement using Computational Restoration (UNFOLD Program) 1993.

Gratier, J.P., Guillier, B., Delorme, A., Odonne, F., 1991. Restoration and balance of a faulted surface by best-fitting of finite elements: principles and applications. Journal of Structural Geology 13, 111–115.

Gratier, J.P., Hopps, T., Sorlien, C., Wright, T., 1999. Recent crustal deformation in Southern California deduced from the restoration of folded and faulted strata. Journal of Geophysical Research 104, 4887–4899.

Hartman, P., Nirenberg, L., 1959. On spherical image maps whose Jacobians do not change sign. American Journal Mathematics 81, 901–920.

Hartman, P., Wintner, A., 1950. On the fundamental equations of differential geometry. American Journal of Mathematics 72, 757–774.

Hartman, P., Wintner, A., 1951. On the asymptotic curves of a surface. American Journal of Mathematics 73, 149–172.

Heck, R.G., 1998. Santa Barbara Channel regional formline map, top Monterey Formation, in: Kunitomi, D.S., Hopps, T.E., Galloway, J.M. (Eds.), Structures and Petroleum Geology Santa Barbara Channel, California, Bakerfield California Pacific Section American Association of Petroleum Geologists, 46, pp. 183–184.

Hopps, T.E., Stark, H.E., Hindle, R.J., 1995. Subsurface data in basin analysis. An example from Ventura basin, California. In: Workshop 'Thrust Ramps and Detachments Faults in the Western Transverses Range', University of Southern California, Santa Barbara Earthquake Center, 10pp.

Hossack, J.R., 1979. The use of balanced cross-sections in the calculation of orogenic contraction: a review. Journal of the Geological Society of London 136, 705–711.

Hupfile, G.J., 1991. Thin-skinned tectonics of the upper Ojai Valley and Sulphur Mountain area, Ventura basin. California American Association of Petroleum Geologists Bulletin 75, 1353–1373.

Jackson, P.A., Yeats, R.S., 1982. Structural evolution of the Carpenteria basin western Transverses Range California. American Association of Petroleum Geologists Bulletin 66, 805–829.

Kamerlin, M.J., Sorlien, C.C., 1999. Quaternary slip and geometry of the Red Mountain and Pitas Point-North Channel faults. California Abs; EOS 46 (80), F1003.

Kerr, H.G., White, N., Brun, J.P., 1993. An automatic method for determining three-dimensional normal fault geometries. Journal Geophysical Research 98, 17837–17857.

Lecomte, J.C., Mondy, J.F., Bennis, C., Léger, M., 1994. A Balanced Surface Method. A New Way to Improve your Structural Maps Interpretation. American Association of Petroleum Geologists Convention, Denver.

Lévy, B., Mallet, J.L., 1998. Non-distorted texture mapping for sheared triangulated meshes. Proceedings of Computer Graphics, Annual Conference Series 1998;, 343–352.

Lisle, R.J., 1992. Constant bed-length folding: three-dimensional geometrical implications. Journal of Structural Geology 14, 245–252.

Morvan, J.M., Thibert, B., 2002. Unfoldings of Surfaces. INRIA's research report, no. 4615.

Ramsay, J.G., 1967. Folding and Fracturing of Rocks. McGraw-Hill, New York. 568pp.

Rouby, D., Xiao, H.B., Suppe, J., 2000. 3-D restoration of complexly folded and faulted surfaces using multiple unfolding mechanisms. American Association of Petroleum Geologists Bulletin 84 (6), 805–829.

Sansom, P., 1996. Equilibrage de structures géologiques 3D dans le cadre du projet GOCAD. Ph.D. thesis, ENSG Nancy, France.

Sheffer, A., De Sturler, E., 2001. Parameterization of faceted surfaces for meshing using angle based flattening. Engineering with Computers 17 (3), 326–337.

Sorlien, C.C., Kamerlin, M.J., 1998. Fault displacement and fold contraction estimated from unfolding of quaternary strata onshore and offshore Ventura basin. California Earthquake Hazard Program. Final report to USGS contract 97-GR-03085, 16pp, digital map scale 1/100,000.

Thibaut, M., Gratier, J.P., Léger, M., Morvan, J.M., 1996. An inverse method for determining three-dimensional fault geometry with thread criterion: application to strike-slip and thrust faults (Western Alps and California). Journal of Structural Geology 18, 1127–1138.

Williams, G.D., Kane, S.J., Buddin, T.S., Richards, A.J., 1997. Restoration and balance of complex folded and faulted rock volumes: flexural flattening, jigsaw fitting and decompaction in three dimensions. Tectonophysics 273 (3-4), 203–218.

Yeats, R.S., 1983. Large-scale Quaternary detachments in Ventura Basin, southern California. Journal of Geophysical Research 88 (B1), 569–583.